Department of Precision and Microsystems Engineering

Active Unit-Cell Structures for Vibration Control:
Conceptual Design of Hexapod Struts

Bryan Rotteveel

Report no : 2022.020
Coach : M.B. Kaczmarek
Professor : S.H. HosseinNia
Specialisation : Mechatronic System Design
Type of report : Master Thesis
Date : June 12, 2022

TU Delft Delft University of Technology

Abstract

In this paper, the implementation of an active unit-cell metamaterial used for vibration control is discussed. The active unit-cell metamaterial is designed for implementation in a hexapod strut. As each of the unit-cells can be sensed and actuated, over-sensing and over-actuation are introduced in the system. This can be used to create vibration isolation behaviour. This is done using the interaction between the unit-cells.
Using the commercial FEM software COMSOL, the amount of unit-cells used in the strut is determined. By looking at the transmissibility of the system, the required controllers are also determined. The presented unit-cell design makes use of simple active damping controllers in order to improve control flexibility for different systems.
The system is validated using a realistic model made in the commercial software Simulink. The model includes sensor dynamics, sensor noise, and a realistic disturbance. By looking at the transmissibility and the disturbance response, the system is compared to an existing solution. Compared to the existing solution, the transmissibility is lowered by at minimum 13 dB in the frequency range of interest. The transmitted disturbance is lowered roughly 20 times with roughly 6.6 times bigger required control effort.

Contents

1 Introduction

One factor with major influence on the precision of high-tech devices is vibrations. Vibrations are always present due to all sorts of processes acting on the surroundings of the high-tech devices. For example, trucks driving past the building in which the high-tech devices are located. The control of these vibrations can significantly improve the precision and thus the performance of high-tech devices.
There are multiple ways of controlling the vibrations inside high-tech devices themselves. This is usually done by controlling the flexible parts inside the devices. They can be controlled by dissipating the vibrational energy using passive methods such as tuned mass dampers. An active system can also be used where Piezoelectric actuators counter the vibrations by making use of a control structure. It is also possible to limit the vibrations coming into the devices from the surroundings. This can be done by making use of a support structure. Such a support is essentially a flexible coupling between the surroundings and the high-tech device. This flexible coupling can be designed and controlled in such a way that the vibrations from the surroundings will have a decreased effect on the precision of the high-tech device.

An example of a support stage is a so-called hexapod. The company 'Physik Instrumente (PI) GmbH & Co' is interested in the use of such a hexapod for vibration control. A hexapod makes use of six struts that can be separately controlled and with their combined effect they can be used to counter the vibrations. The setup that will be used in this paper, can be seen in Figure 1.

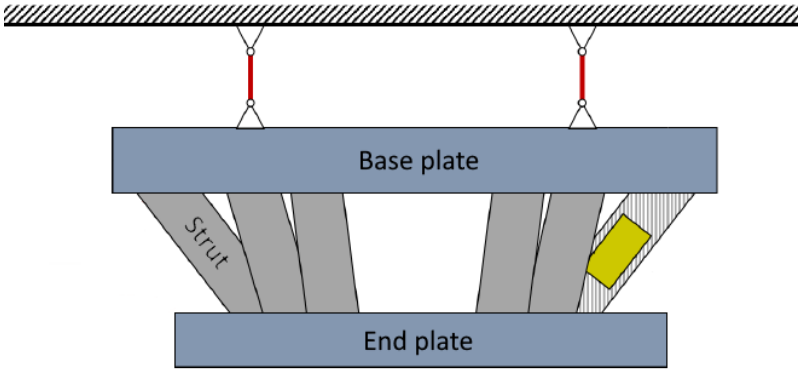

Figure 1: The hexapod structure setup used for the problem in this paper

As can be seen in Figure 1, the setup consists of a base plate suspended from the ceiling. The base plate is connected to the end plate via six axially loaded one-dimensional struts. As the end plate symbolizes the to-be-controlled system, the six struts are used for the vibration control. The struts make use of a Piezoelectric stack actuator for the vibration control. This can be seen in Figure 2.

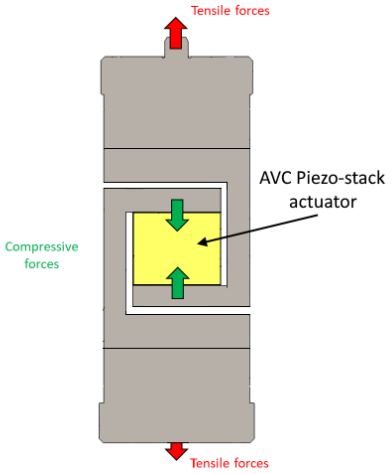

Figure 2: The strut as designed with current solutions

The solution for these struts that has been presented makes use of a Piezoelectric stack actuator that can be actuated and controlled for the purpose of vibration control. The struts are controlled using a Direct-Velocity-Feedback (DVF) controller. Such a controller is able to control the resonances in the system given that the controller is acting on a collocated system. While this setup is able to control the resonances in the system quite well, better disturbance rejection and added control flexibility for different systems is desired. The implementation of model-based controllers has been researched in literature as well [1], where an adaptronic rod is used for vibration control. This system is able to show improved tracking behaviour and better disturbance rejection due to the implemented model-based controller. However, for the use of such a model-based controller, the system dynamics need to be known quite well. Thus, this limits the control flexibility for different systems.

The implementation of metamaterials has proven an interesting solution for vibration control. With metamaterials, the typical properties of materials can be altered in such a way that the material becomes better suited for vibration control. This can be done using various passive methods using local resonance or Bragg scattering [2], or shunts [3]. But also using active methods making use of Piezoelectric actuators [4].
One particularly interesting metamaterial implementation is the implementation of active unit-cells [5], where the material will be build out of cells. By controlling these cells in such a way that they are interacting with each other, it is possible to create vibration isolation behaviour. This method works because of added over-sensing and over-actuation [6]. This over-sensing and over-actuation improves the observability and the controllability of the system respectively, which will be used for the vibration control.

Thus, this paper presents the implementation of an active unit-cell type metamaterial into one-dimensional longitudinal struts. Such that over-sensing and over-actuation lead to a better observability and controllability of the system. Which in turn improves the vibration control and adds control flexibility for different systems.
The problem will be discussed in more detail and the solution given by the unit-cells is presented. By making use of modelling the system dynamics will be presented. The structure of the unit-cell setup will be designed and tested in COMSOL. A control system will

be designed as well. The designed setup will be implemented in a realistic model and tested. Simulink is used to create this realistic model by implementing sensor dynamics, sensor noise, and a realistic disturbance signal. The transmissibility and the disturbance rejection of the system will be compared to the current solution. The cost of the implementation of the unit-cell system will be tested as well by presenting the control effort. In the end, it is concluded that the unit-cell system shows improved transmissibility and improved disturbance rejection at the cost of a more complex system.

2 Background Knowledge

To create an understanding of the existing solution, the system dynamics of the presented setup will be explained in more detail first. After this, the working principle of the unit-cell type metamaterial will be presented in more detail. This is done to create an understanding of the implementation of the unit-cells into the one-dimensional longitudinal struts. Since Matlab is used for some of the derivations, the used Matlab codes are added in Appendix B.

Existing solution

The hexapod given in Figure 1 makes use of six one-dimensional struts that are loaded in tension. These struts make use of Piezoelectric stack actuators and are controlled using Direct-Velocity-Feedback (DVF) controllers. The signal used to create the proper control is given by six one-dimensional accelerometers mounted coaxially with each of the six struts. On top of this, three three-dimensional accelerometers are present on the surface of the end plate. By using a combination of the actuators, the controllers, and the various sensors, the vibrations of the end plate are controlled.

Since the implementation of the unit-cells into the struts is mainly of interest, the setup will be limited to one such strut, which can be seen in Figure 2. It is assumed that such a strut makes use of the coaxially mounted one-dimensional accelerometer only. This assumption is made as the control of the entire hexapod is not of interest, thus only the control of one strut will be considered. Together with the one-dimensional coaxially mounted accelerometer, a collocated system is created.
This system can be tested by isolating one strut and applying a load to it at the end. This load will be given by a mass of 80kg. Consider the strut as a mass-spring system with an actuator acting on the mass as well, presented in Figure 3. The spring stiffness in this case is equal to the stiffness of the strut, which is known to be 170 N/μm, and the mass is equal to the 80kg. The actuator can be presented by a force actuator.

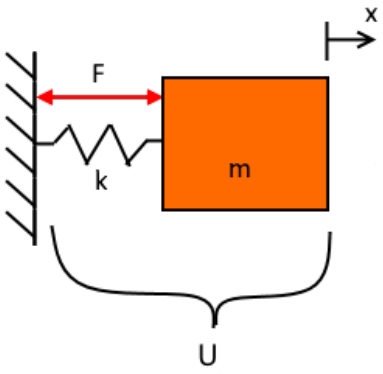

Figure 3: The mass-spring system approximation of the strut

Assuming that there is no damping in the system, it can be derived easily that the transmissibility of disturbance d of this strut is equal to:

$$T_{strut} = \frac{x}{d} = \frac{k}{ms^2 + k} \tag{1}$$

Where x is the end position, k is the stiffness of the strut, m is the mass of the load, and s is the Laplace variable.
By now implementing DVF control, the force actuator will be delivering the following force on the system:

$$F = \frac{-ga}{s} \tag{2}$$

Where g is the gain of the DVF controller, a is the acceleration of the load, and s is again the Laplace variable.
When the control is active, the transmissibility of the system changes to:

$$T_{strut,c} = \frac{x}{d} = \frac{k}{ms^2 + gs + k} \tag{3}$$

By comparing Equation 3 to Equation 1 it can easily be seen that the DVF controller adds damping to the system. Thus, the existing solution is able to dampen the resonance in the system. However, it is unable to lower the overall transmissibility. The added damping is thus also not able to present a lowering of the transmitted vibrations. Since the presented hexapod will be used as a support structure, its function will be to limit the effect of outside vibrations coming into the system. Thus, the lowering of the transmitted vibrations is desired.
In order to limit the vibration transmissibility in the system, the implementation of active unit-cells is presented.

Unit-cell solution

Consider a multiple unit-cell system where the unit-cells are connected in series presented in Figure 4. Assume that the unit-cell system is connected to the ground on one end and connected to a load on the other end.

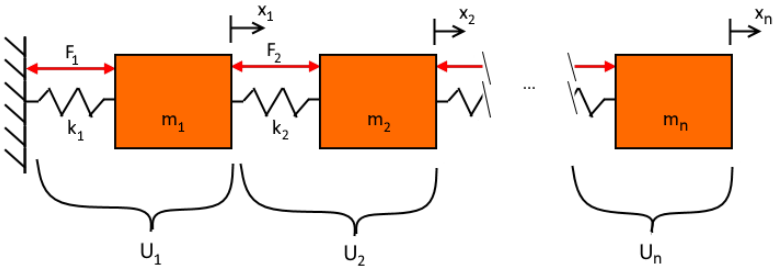

Figure 4: A multiple unit-cell system where 'n' denotes the total number of unit cells

The dynamics of such a system can be approximated by a multiple-mass-spring system where each unit-cell has its own stiffness and its own mass. On top of this, each unit-cell can provide a force between its own mass and the mass of the previous unit-cell. Each unit-cell also has its own sensor. For ease of deduction, it is assumed that the system contains two unit-cells. However, it can easily be seen that the system works for more unit-cells as well. In order to check the system dynamics, the following equations of motions are used in order to determine the transfer functions:

$$\begin{bmatrix} m_1 & 0 \\ 0 & m_2 \end{bmatrix} \begin{bmatrix} x_1 \\ x_2 \end{bmatrix} s^2 = \begin{bmatrix} F_1 - F_2 \\ F_2 \end{bmatrix} + \begin{bmatrix} -k_1 - k_2 & k_2 \\ k_2 & -k_2 \end{bmatrix} \begin{bmatrix} x_1 \\ x_2 \end{bmatrix} \tag{4}$$

Here, s is the laplace variable.

Solving these equations for each input F_n and each output x_n (while stating that the other inputs are zero) gives the following transfer functions:

$$G_{11} = \frac{x_1}{F_1} = \frac{m_2 s^2 + k_2}{k_1 k_2 + (k_1 m_2 + k_2 m_1 + k_2 m_2) s^2 + (m_1 m_2) s^4} \tag{5}$$

$$G_{12} = \frac{x_2}{F_1} = \frac{k_2}{k_1 k_2 + (k_1 m_2 + k_2 m_1 + k_2 m_2) s^2 + (m_1 m_2) s^4} \tag{6}$$

$$G_{21} = \frac{x_1}{F_2} = \frac{-m_2 s^2}{k_1 k_2 + (k_1 m_2 + k_2 m_1 + k_2 m_2) s^2 + (m_1 m_2) s^4} \tag{7}$$

$$G_{22} = \frac{x_2}{F_2} = \frac{m_1 s^2 + k_1}{k_1 k_2 + (k_1 m_2 + k_2 m_1 + k_2 m_2) s^2 + (m_1 m_2) s^4} \tag{8}$$

Here, G_{nm} is the transfer function of input F_n to output x_m.

These transfer functions can now be used in the following equation which can be used to determine the output given certain inputs:

$$\begin{bmatrix} x_1 \\ x_2 \end{bmatrix} = \begin{bmatrix} G_{11} & G_{21} \\ G_{12} & G_{22} \end{bmatrix} \begin{bmatrix} F_1 \\ F_2 \end{bmatrix} \tag{9}$$

In order to check the response of the system to an external disturbance d coming into the system from the ground, the following force input can be used:

$$F_1 = dk_1 \tag{10}$$

Given this input (Equation 10), the transmissibility of the uncontrolled system can be found to be:

$$T_s = \frac{x_2}{d} = k_1 G_{12} \tag{11}$$

Unit-cell control

With the system dynamics known for an unactuated system, control can be added in order to create vibration isolation behaviour. To achieve this behaviour, the unit-cells need to cancel each other's vibrations. For this to happen, the second unit-cell needs to have the same displacement as the first unit-cell, however it needs to have opposite sign. This is done by using the second force actuator to create this displacement. The required force is determined by first measuring the displacement signal at the mass of the first unit-cell. This signal is then multiplied by a gain equal to the stiffness of the second unit-cell, which creates the force signal:

$$F_2 = -x_1 k_2 \tag{12}$$

This uses the same principle as the transmissibility to compliance coupling (Equation 10). The block diagram of this system can be seen in Figure 5.

Looking at the disturbance and the control filled in into Equation 9:

$$\begin{bmatrix} x_1 \\ x_2 \end{bmatrix} = \begin{bmatrix} G_{11} & G_{21} \\ G_{12} & G_{22} \end{bmatrix} \begin{bmatrix} dk_1 \\ -x_1 k_2 \end{bmatrix} \tag{13}$$

Gives:

$$x_1 = G_{11} dk_1 - G_{21} x_1 k_2 \tag{14}$$

And:

$$x_2 = G_{12} dk_1 - G_{22} x_1 k_2 \tag{15}$$

Solving these equations leads to the following transmissibility function:

$$T_{s,c} = \frac{x_2}{d} = k_1 (G_{12} + G_{22} G_{11} \frac{-k_2}{1 + k_2 G_{21}}) \tag{16}$$

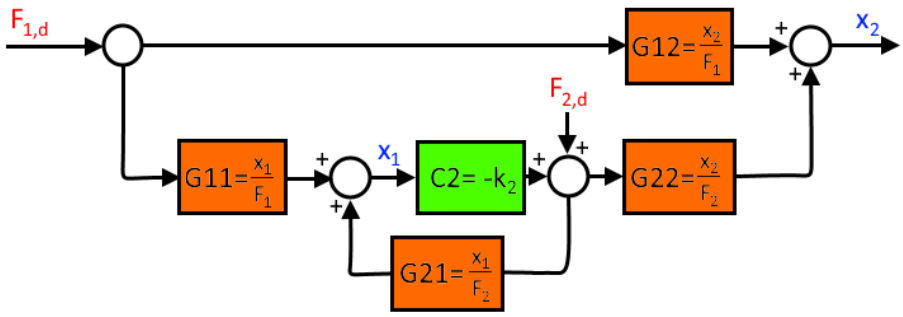

Figure 5: The block diagram of the controlled system; $F_{1,d}$ and $F_{2,d}$ can be used to insert disturbances into the system in each respective unit-cell

Unit-cell transmissibility

The previously derived transmissibilities are now plotted without control, with non-ideal control, and with ideal control. This can be seen in Figure 6.

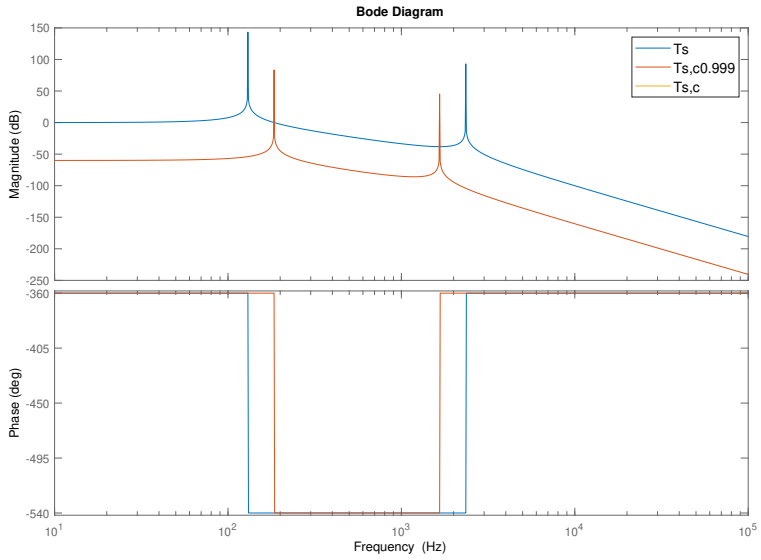

Figure 6: The transmissibility of the uncontrolled and the controlled system; here T_s is the uncontrolled system, $T_{s,c0.999}$ is the controlled system with an 0.1% error in the gain, and $T_{s,c}$ is the fully controlled system; since the transmissibility of $T_{s,c}$ is zero, it can not be seen in the plot

As can be seen from Figure 6 looking at the yellow line, the control indeed removes transmissibility from the system as the theory stated. This can be seen as the transmissibility of the yellow line is equal to zero and thus is not plotted in the Bode diagram. It can also be seen that once the control has only a slight error from the ideal gain, the transmissibility is still lowered significantly but full vibration isolation can no longer be realised. This behaviour is understandable as with the imperfect control, the vibrations can still be transmitted to the end-load, albeit lessened. The actual impact of the control gain can be seen in the transmissibility when Equation 16 is worked out and the control gain is kept a variable:

$$T_{s,c} = \frac{k_1(k_2 + k_c)}{k_1k_2 + k_1m_2s^2 + k_2m_1s^2 + k_2m_2s^2 + k_cm_2s^2 + m_1m_2s^4} \tag{17}$$

Here, k_c is the controller gain.

As can be seen from Equation 17, once $k_c = -k_2$, the numerator becomes zero. Which results in a zero transmissibility. However, a slight error in the gain with respect to the ideal gain causes the numerator to be a non-zero value. Thus, the vibrations can be transmitted for non-ideal gain.

It can also be seen from Figure 6 that although vibration isolation can be introduced by the interaction of the unit-cells, the resonances are still undamped. This means that the

modes of the system can still be excited which will result in less precision. In order to also dampen the modes, the unit-cells would also need to be controlled by an additional controller.

3 Setup

In order to see the effect of the implementation of the active unit-cells, it needs to be compared to the existing solution. First, the structure of the strut needs to be redesigned with multiple unit-cells. While the design could be altered significantly, it is chosen to keep a similar design as also presented in Figure 2. This design can then be shrunk and be implemented multiple times in series. By doing this, unit-cells become available for the control. A COMSOL study is carried out in order to assess the changes these unit-cells make to the passive behaviour of the strut.

Structure

For the two systems to be a fair comparison, the systems need to be alike as much as possible. The parameters that will likely change due to the implementation of the unit-cells are: the stiffness, the displacement capability of the Piezoelectric material, and the amount of resonances and modes in the system. The introduction of unit-cells into the structure of the strut adds modes to the system. As these modes can be controlled and as the effect of unit-cells is of interest, the additional modes will not be considered a design limitation. The introduction of unit-cells also influences the stiffness of the strut directly as the unit-cells are connected in series. Thus, the lower stiffness of the system will also not be considered a design limitation. If needed, the stiffness can also be adjusted using control. Finally, the displacement capability of the Piezoelectric material does pose a limitation on the system. The systems are desired to behave similarly when introducing a certain level of control. Thus, it is required of the unit-cell system to have a similar displacement as the existing solution, given a constant voltage.
In order to present the best design, the amount of unit-cells can be changed to see its impact on the previously mentioned parameters of the system. The outer dimensions of the design space for the actuating part of the strut are kept constant. As well as the diameters of the Piezoelectric material. This is done as the unit-cells stack in series, thus the change in height of the unit-cells is more significant than a change in diameter of the Piezoelectric material would be. Finally, the supporting structure is constant for the unit-cell setups as the supporting structure needs to house some necessary parts. The actual dimensions can be found in Appendix A.

The study that is carried out compares the stiffness and the displacement as previously mentioned between various amounts of unit-cells. An example of a unit-cell setup compared to the existing setup can be seen in Figure 7.

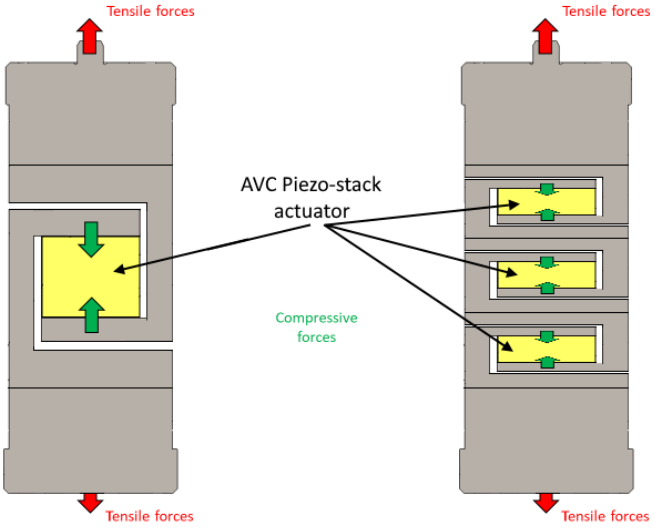

Figure 7: A schematic of the original strut to the left and a three unit-cell strut to the right

The comparison of various amounts of unit-cells between one and four can be seen in Table 1. Here, the one unit-cell setup is the original setup.

Amount of unit cells	**Stiffness**	**Displacement (500V)**	**Total Piezo height**
Original	552 N/μm	8.7 μm	39 mm
2 Cells	218 N/μm	12.6 μm	61 mm
3 Cells	171 N/μm	7.3 μm	44 mm
4 Cells	140 N/μm	4.4 μm	27 mm

Table 1: Amount of unit cells

As can be seen from Table 1, the more unit-cells are implemented the less stiffness the struts seems to have. The same principle can be seen for the amount of Piezoelectric material (Piezo height) that is available in each setup. Only the original setup does not fit in this trend. This is because in the original setup, more space is used for the structural support of the Piezoelectric material. Finally, it can be seen that the displacement depends on the amount of available Piezoelectric material.
The three unit-cell setup maximizes the amount of unit-cells while still being reasonably close to the amount of displacement of the original setup. Thus, it can be concluded that three unit-cells are the best option. It should however be noted that the unit-cell setups have less support structure for each unit-cell than the original case would have. This is elaborated on in Appendix A.

As previously mentioned, unit-cells do also present additional modes and resonances. Thus, it is of interest to check the system dynamics in order to get an understanding of the dynamical behaviour of the setup. Looking back at the system dynamics of the unit-cells as presented in section 2, each unit-cell adds a mass-spring system to the dynamical behaviour. Thus, the three unit-cell system acts as a three mass-spring system. This presents the issue of two additional resonances in the system compared to the original setup which must be solved.

Control

In order to control the system, multiple controllers can be implemented. As control flexibility for different systems is desired, the more easily implementable active damping controllers are of interest. The controller used in the original setup is a DVF controller. The DVF controller is capable of adding damping to the resonances in the system. This controller is able to control the added resonances in the three unit-cell setup.
However, while this dampens the resonances, the added value of the implementation of unit-cells will not be adressed by these controllers. Thus, the control as mentioned in the control section of section 2 will also be implemented.

Since multiple controllers are of interest for the three unit-cell setup, combining the controllers is of interest. The principle of combining these controllers is explained in literature [7]. It states that multiple sensor-controller systems can be combined in order to create combined control for the same unit-cell. Thus, this principle will also be used in the presented three unit-cell setup.

4 Method

For validation, a simulation is used in order to check the system under realistic circumstances. For this simulation, Simulink is used.

Similar to the theory, the unit-cells will be modelled by a multiple-mass-spring system. For this, each unit-cell is implemented as a force actuator with an internal stiffness which is connected to a mass. This can be seen in Figure 8.

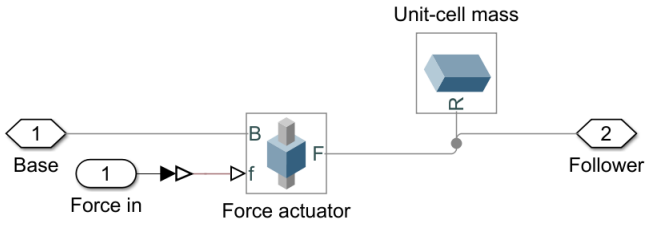

Figure 8: The mass-spring model of the unit-cell as implemented in Simulink

These unit-cells are then connected in series. They are connected to the ground on one end and to the load at the other end. This way they simulate the entire strut with load. A separate sensor is introduced for each unit-cell that will be able to measure the acceleration of each unit-cell with respect to the world. Thus the used sensors will be collocated and absolute. This can be seen in Figure 12.

As the realistic response of the system is desired, the sensor dynamics will also be implemented. This means that the sensor will show an upper bandwidth. This will be implemented by adding a second order low-pass filter to the signal. When the acceleration signal is integrated as will be the case for the velocity and the position signal, the

low frequencies of accelerometers can cause stability issues. Which is why also a lower bandwidth of the accelerometers is implemented. This can be done by substracting the lower frequencies from the signal using a second order low-pass filter (or by simply adding a second order high-pass filter). Now the signal within the bandwidth of the accelerometer is known. However, this is still not a realistic representation of the sensor as sensor noise is always present. This will be implemented by using band-limited white noise. It is important that the amplitude of this noise is tuned to realistic values. Now, this noise can be simply added to the acceleration signal before the sensor dynamics. This can be seen in Figure 9.

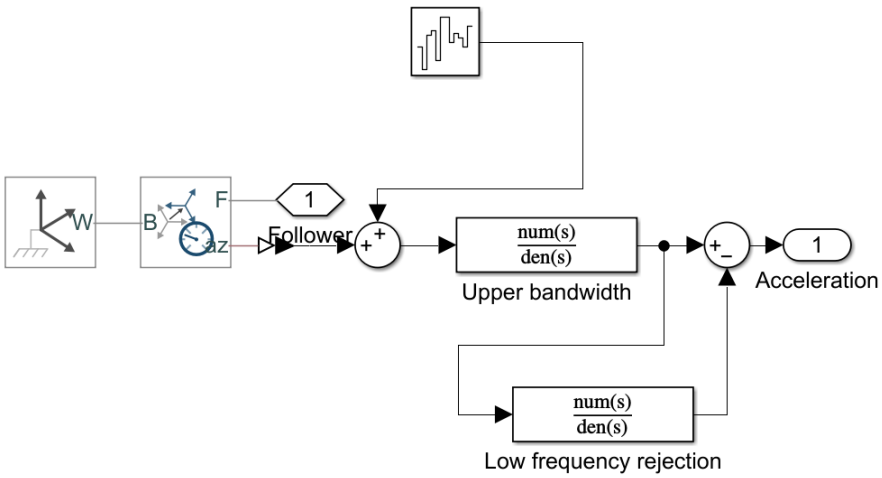

Figure 9: The sensor with sensor dynamics and sensor noise taken into account as implemented in Simulink

A similar model is created for the original setup. However, this time the setup only consists of one 'unit-cell' as can be seen in Figure 13.

The unit-cell system makes use of three controllers of which one combined controller. It uses three DVF controllers at each unit-cell in order to dampen the resonances created by the three mass-spring system. The DVF controller can be seen in Figure 10. Next to this a Negative-Position-Feedback (NPF) controller is used with the unit-cell interaction principle as presented in section 2. The NPF controller can be seen in Figure 11. This controller is implemented between the first and the second unit-cell and combined with the second DVF controller. The overall controller setup of the unit-cell system can be seen in Figure 12.
The original setup only makes use of a DVF controller. This can be seen in Figure 13.

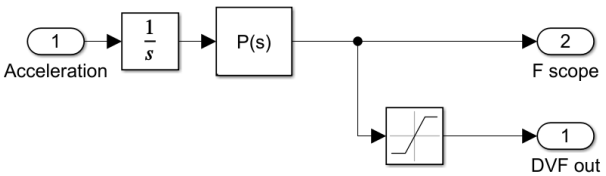

Figure 10: The DVF controller as implemented in Simulink

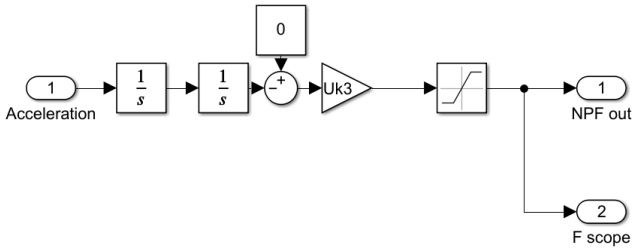

Figure 11: The NPF controller as implemented in Simulink

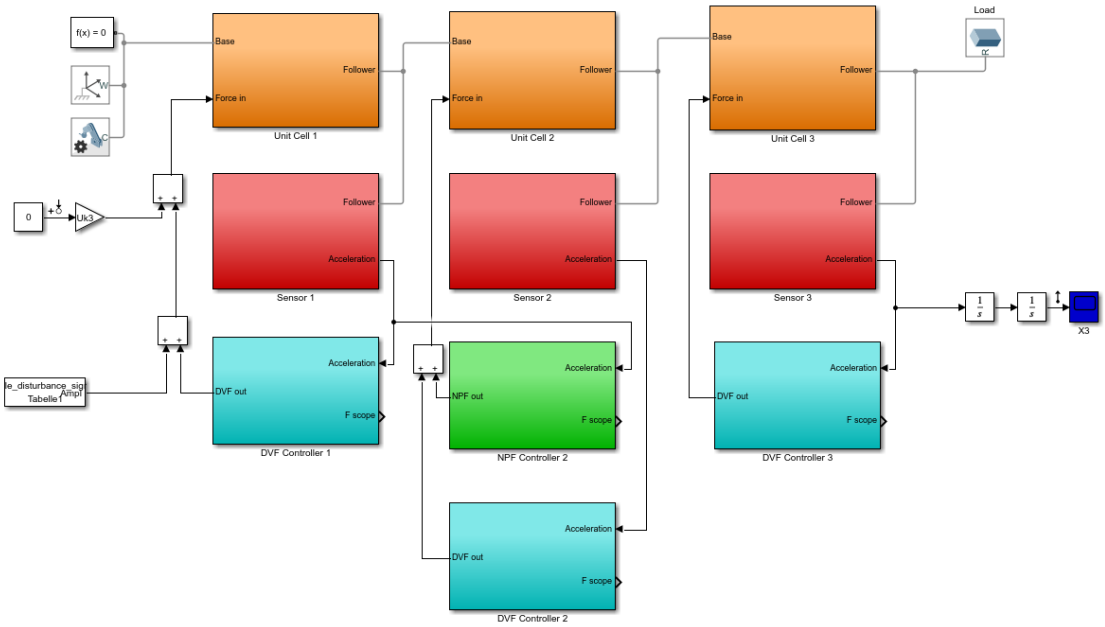

Figure 12: The unit-cell system including sensors and controllers as implemented in Simulink

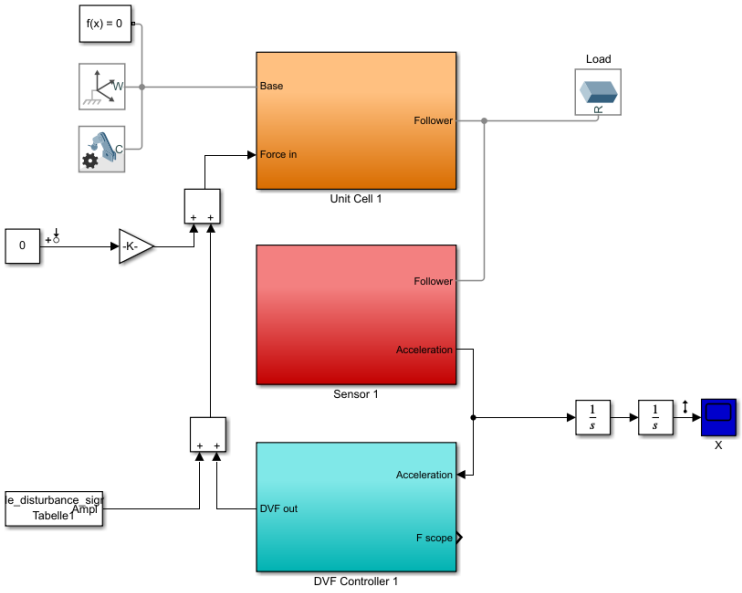

Figure 13: The original system including sensors and controllers as implemented in Simulink

This model can now be used in order to check the transmissibility of both systems. This is done using the model linearizer of Simulink. An input perturbation is created at a signal which is fed to the first force actuator. A gain is applied to this signal, equal to the stiffness of the first unit-cell. This uses Equation 10. The output of this perturbation is then measured at the end position of the system.

While the frequency responses of the system are interesting as it gives an indication of the performance of the system, the time response is also important. The time response presents the disturbance rejection of the system. In order to test this disturbance rejection, a disturbance signal provided by PI is acting on the system. The time response can then simply be seen.
The required force in order to control this disturbance can also be seen by using the 'Fscope' signals each controller outputs.

Finally, the step response is given as well. This step response is again created using the model linearizer of Simulink using the same setup as described previously.

5 Results and Discussion

Transmissibilities

As previously mentioned, one of the results is the transmissibilities of the the original system and of the unit-cell system. The transmissibility of the unit-cell system will be compared to the theoretical transmissibility of the unit-cell system. This theoretical transmissiblity is determined similarly to the two unit-cell system presented in section 2. The codes used to obtain this theoretical transmissibility can be found in Appendix B.

The theoretical results of the unit-cell system can be seen in Figure 14. Here, three

transmissibilities are given, the transmissibility without control, the transmissibility with non-ideal control, and the transmissibility with ideal control. The transmissibility with non-ideal control is added as the effect of the DVF controllers can then be seen. The ideal control results in a zero transmissibility.

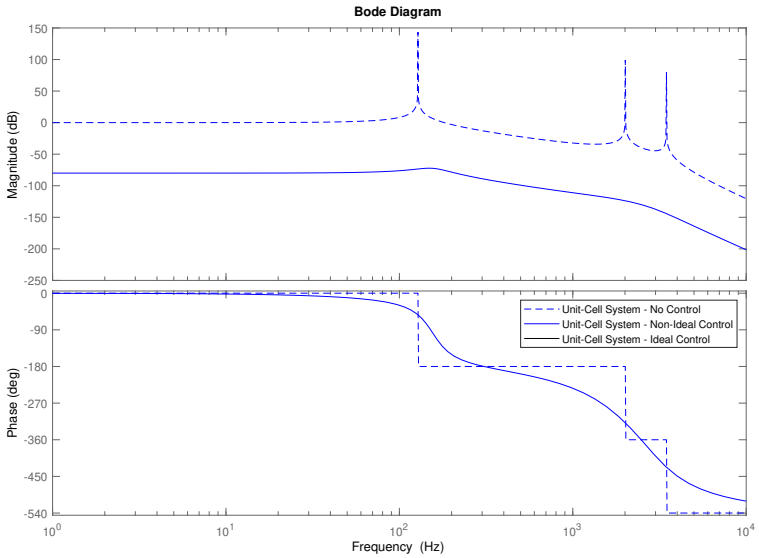

Figure 14: The theoretical transmissibilities of the unit-cell system

The transmissibilities of the realistic model compared to the theoretical results can be seen in Figure 15. Here it can be seen that the ideal control of the system no longer creates total vibration isolation when the realistic model is taken into account. It can also be seen that the uncontrolled systems do not perfectly match, which is due to the sensor bandwidth.

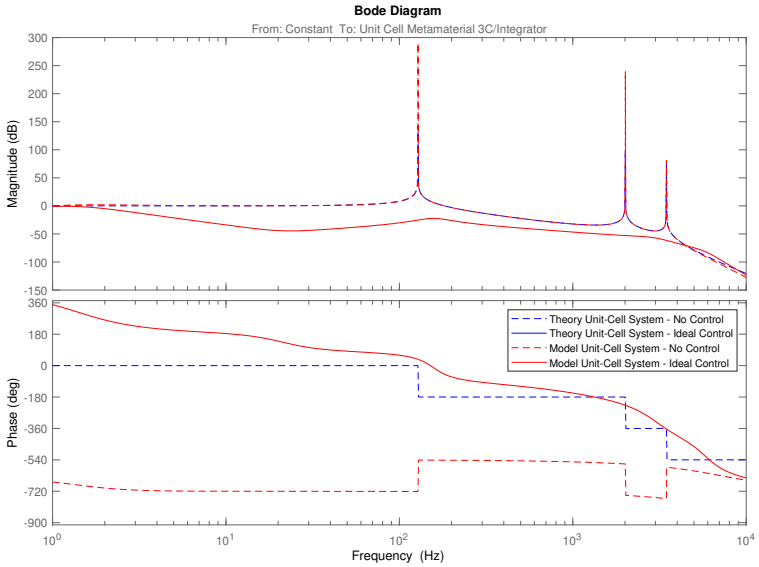

Figure 15: The theoretical transmissibilities of the unit-cell system in blue compared to the transmissibilities of the realistic model of the unit-cell system in red

The transmissibilities of the realistic model of the unit-cell system compared to the realistic model of the original system can be seen in Figure 16. Here it can be seen that the original system only damps the resonance, while the unit-cell system damps the resonances next to showing vibration isolation behaviour. Looking at Figure 16, it can be concluded that from approximately 3 Hz onwards, the unit-cell system shows a decrease of at the least approximately 13 dB compared to the original system.

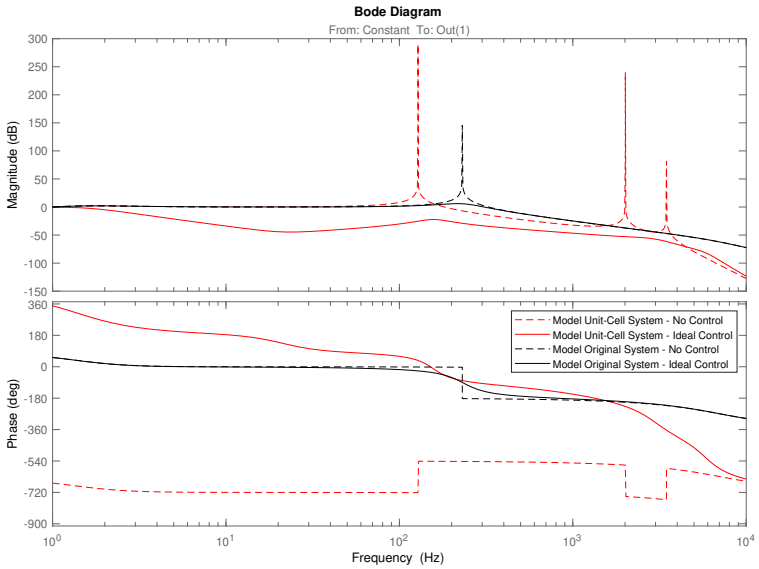

Figure 16: The transmissibilities of the realistic model of the unit-cell system in red compared to the transmissibilities of the realistic model of the original system in black

Time response

Given the force disturbance signal as can be seen in Figure 17, the responses of both the realistic unit-cell system and the original system can be seen in Figure 18. Here, it can be seen that the disturbance rejection of the unit-cell system is significantly more effective than the disturbance rejection of the original system. It can also be seen that the displacement signals of both systems seem to drift away from the starting position. This is due to the noise being integrated. It can be stated however that if the Signal-to-Noise-Ratio (SNR) is sufficient, this will not pose a significant problem.
Using the Root-Mean-Square (RMS) value of the signals, a comparison in terms of performance can be drawn. For this, the drift-like behaviour will be excluded as it does not show the disturbance rejection of the system. It can be stated using this method that the unit-cell system shows a roughly 20 times increase in disturbance rejection compared to the original system.

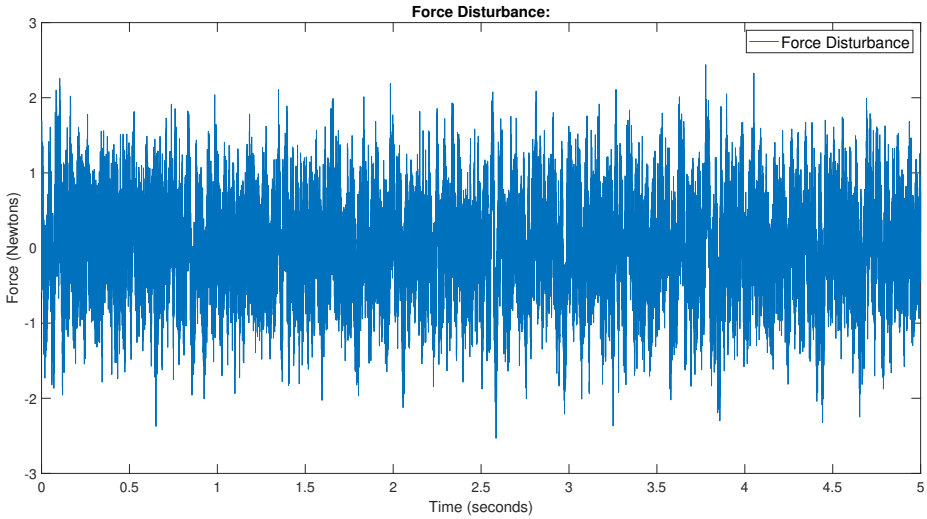

Figure 17: The force disturbance acting on the system

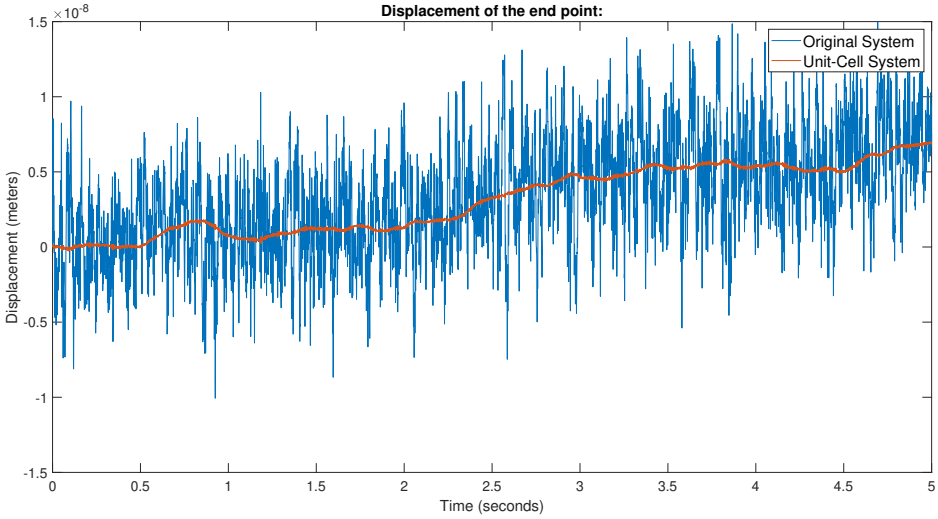

Figure 18: The time response after a disturbance of the original system in blue and the unit-cell system in orange

The required force in order to control the disturbance acting on the system can be seen in Figure 19. As can be seen, the unit-cell system requires more force in order to control the disturbance on the system. On top of this, the unit-cell system seems to react to the drift more than the original system. Again the RMS value is used to compare the systems. However, this time the drift is taken into account as the unit-cell system reacts to it. It can be stated using this method that the required force of the unit-cell system is roughly 6.6 times as high as the original system. Given the increase in disturbance rejection of 20 times, this increase in required force is not proportional. Thus, the unit-cell system shows a relative improvement in performance.
It is noted that the required control force of the unit-cell system can vary based on the drift-like behaviour of the system due to noise. As noise is random, the drift-like behaviour will also show random patterns. In turn, the control force of the unit-cell system also changes at random.

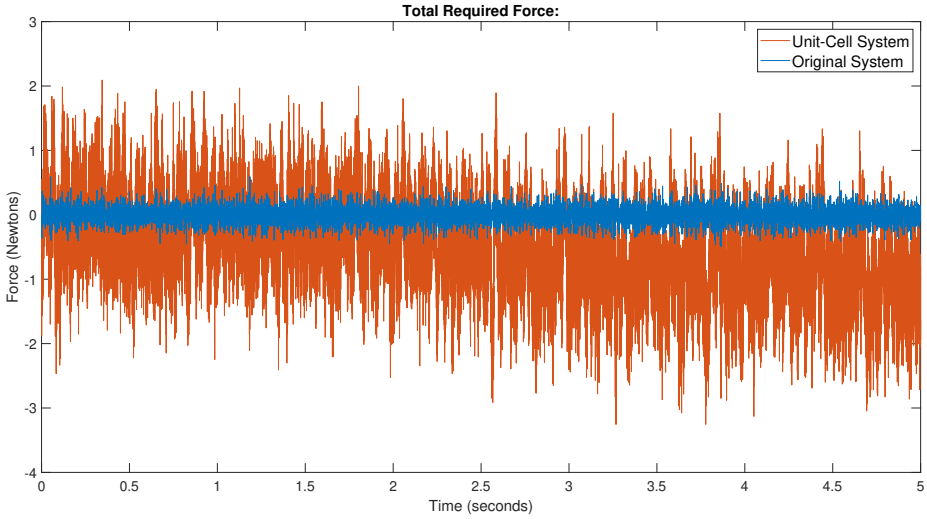

Figure 19: The total force required in order to create the time response as seen in Figure 18 with the original system in blue and the unit-cell system in orange

Finally, the step response of the system can be seen in Figure 20. It can be seen that the unit-cell system again is better at rejecting this step disturbance. The step response of the unit-cell system has a peak value of 0.535 compared to a peak value of the original system of 1.43. However, the unit-cell system is slower in terms of the settling time. The unit-cell system has a settling time of 1.01 seconds, while the original system has a settling time of 0.622 seconds. Both settling times are measured from zero seconds.

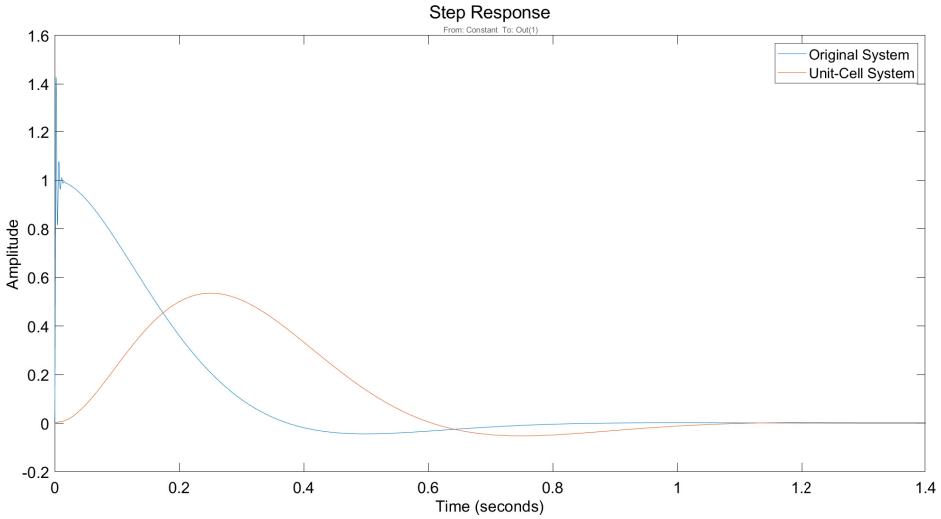

Figure 20: The step response of the original system in blue and the unit-cell system in orange

6 Conclusion

In this paper, the implementation of an active unit-cell type metamaterial into one-dimensional longitudinal struts is discussed. The original system only used one controlled cell which made use of a DVF controller which was able to dampen the resonances in the system. Contrary to this, the unit-cell type metamaterial makes it possible to create vibration isolation in the struts. This is done through added observability and controllability in the system by making use of a sensor and an actuator in each unit-cell. The interaction between these unit-cells has been shown to inhibit vibration isolation behaviour when using the right controller. This controller is a NPF controller that makes use of the signal of one unit-cell in order to control the next-in-line unit-cell. The control gain is very important as it is shown that non-ideal control removes the total vibration isolation behaviour. However, even with non-ideal control it is able to show a significant decrease in the transmissibility. The need to also implement DVF controllers in order to dampen the resonances of the system was noted.
By making use of a simple multiple mass-spring system with added sensors and actuators, the system dynamics were modelled. By adding sensor dynamics, sensor noise, and a realistic disturbance to this model, the system could be tested in a realistic manner.

It can be concluded that the presented unit-cell implementation shows a lower transmissibility over the entire frequency range of interest as it shows at minimum an approximately 13 dB decrease compared to the original system. This also resulted in better disturbance rejection of the unit-cell system with a roughly 20 times decrease in transmitted disturbance. This better disturbance rejection was created with a roughly 6.6 times bigger required control effort. Thus, it can be stated that the unit-cell system shows better performance given its control effort. It should be noted however, that the implementation of unit-cells into the system makes for a more complex system as well. This is both the case in terms of the structure and in terms of the controller setup.

The implementation of the unit-cell system as presented in this paper showed some promising improvements on existing solutions. However, the interaction between the unit-cells can be explored in more detail in future work. This could include other controllers or various combinations of unit-cell interactions.
On top of this, the structure of unit-cells could be studied in more detail as its more complex nature could present problems regarding manufacturability.

Bibliography

[1] Alexandra Ast et al. "An adaptronic approach to active vibration control of machine tools with parallel kinematics". In: *Production Engineering* 3 (2 June 2009), pp. 207–215. ISSN: 09446524. DOI: 10.1007/s11740-008-0142-0.

[2] Srajan Dalela, P. S. Balaji, and D. P. Jena. "A review on application of mechanical metamaterials for vibration control". In: *Mechanics of Advanced Materials and Structures* (Feb. 2021), pp. 1–26. ISSN: 1537-6494. DOI: 10.1080/15376494.2021.1892244.

[3] J. A.B. Gripp and D. A. Rade. "Vibration and noise control using shunted piezoelectric transducers: A review". In: *Mechanical Systems and Signal Processing* 112 (Nov. 2018), pp. 359–383. ISSN: 10961216. DOI: 10.1016/j.ymssp.2018.04.041.

[4] P. Shivashankar and S. Gopalakrishnan. "Review on the use of piezoelectric materials for active vibration, noise, and flow control". In: *Smart Materials and Structures* 29 (5 May 2020). ISSN: 1361665X. DOI: 10.1088/1361-665X/ab7541.

[5] Amit Singh, Darryll J. Pines, and Amr Baz. "Active/passive reduction of vibration of periodic one-dimensional structures using piezoelectric actuators". In: *Smart Materials and Structures* 13 (4 Aug. 2004), pp. 698–711. ISSN: 09641726. DOI: 10.1088/0964-1726/13/4/007.

[6] Thomas Van Der Graaf. *Active Vibration Control Using over-sensing and over-actuation.* Aug. 2020. URL: http://repository.tudelft.nl/..

[7] D. Tjepkema. "Active hard mount vibration isolation for precision equipment". English. PhD thesis. Netherlands: University of Twente, Nov. 2012. ISBN: 9789036534185. DOI: 10.3990/1.9789036534185.

A Appendix A: COMSOL Model and Manufacturability

In this appendix the COMSOL model as well as the parameters used in and gained from the model are presented.

A simplified COMSOL version of the original strut can be seen in Figure 21. The dimensions of the strut can be seen in Table 2. The locations of the components mentioned can be found in Figure 22.

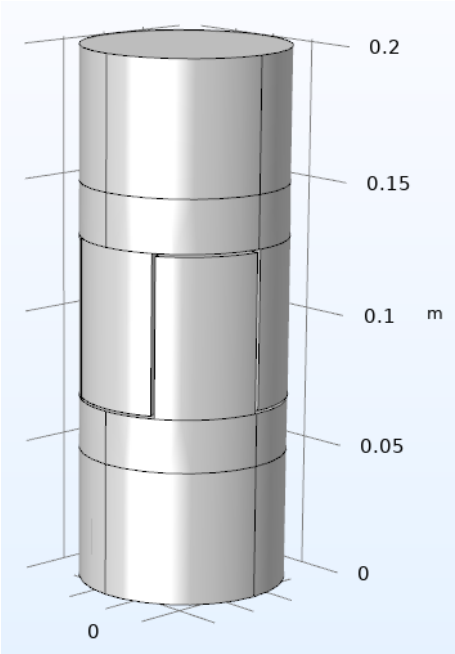

Figure 21: A simplified COMSOL version of the original strut

Component	Size
Strut Length	198 mm
Strut Diameter	78 mm
Design space - Height	100 mm
Design space - Diameter	78 mm
Actuator Height	39 mm
Actuator Diameter	45 mm
Clamping lip thickness	10 mm
Support structure height	20 mm

Table 2: The dimensions of the original strut

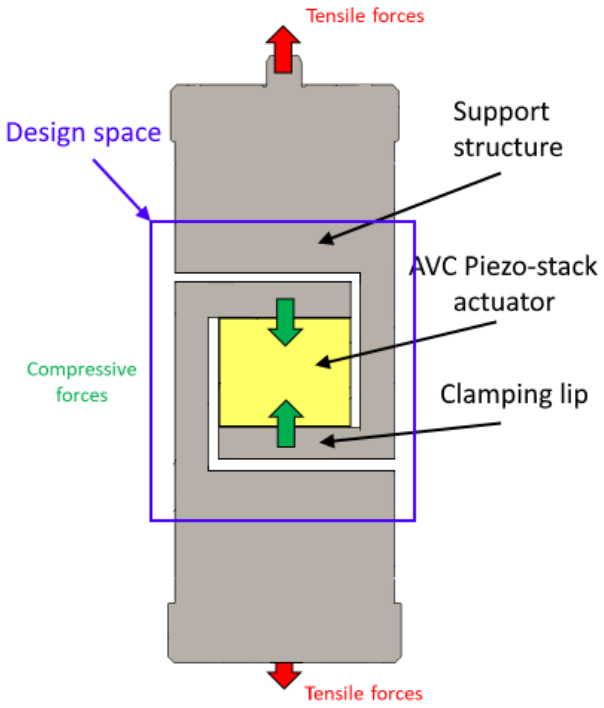

Figure 22: The locations of the components as mentioned in Table 2

As can be seen in Figure 21, the clamping of the Piezoelectric actuator is done using six 'fingers' where three fingers of the bottom interlace with three fingers from the top. It can also be seen that the support structure for the actuator has a height of 20 mm. This height is used for the implementation of a disk spring that will make sure the Piezoelectric actuator is always in compression even when the strut is not loaded. On top of this, this space is used to implement the bolts used to connect all the various components the entire strut is built up from. Finally the clamping lip is 10 mm thick. This lip is used to clamp the actuator and its thickness has an influence on the stiffness of the strut.

The chosen unit-cell setup makes use of three unit-cells which are essentially shrunken versions of the design space of the original strut. The COMSOL model for this can be seen in Figure 23. The dimensions of the unit-celled strut can be seen in Table 3.

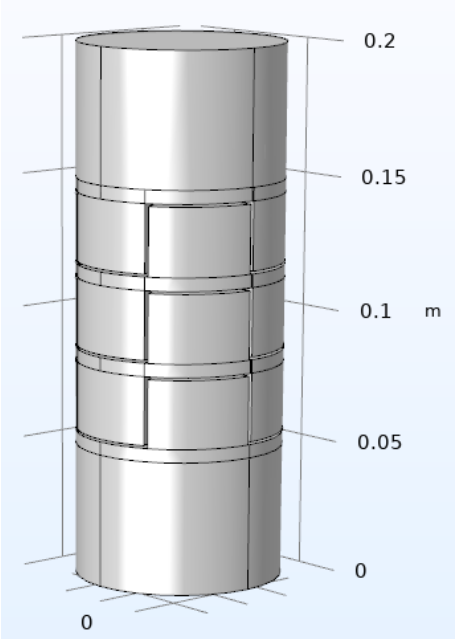

Figure 23: A simplified COMSOL version of the unit-celled strut

Component	Size
Strut Length	198 mm
Strut Diameter	78 mm
Design space - Height	100 mm
Design space - Diameter	78 mm
Total actuator Height	44 mm
Actuator Diameter	45 mm
Clamping lip thickness	5 mm
Support structure height	5 mm

Table 3: The dimensions of the unit-celled strut

As can be seen in Figure 23, the three unit-cells are indeed smaller versions of the design space of the original strut. However, in order to realise this, the support structure had to be shrunk a lot. The clamping lip also had to become thinner.
The thinner clamping lip mainly influences the stiffness of the individual unit-cells. However, the biggest decrease in stiffness of the unit-celled strut is due to the unit-cells being placed in series. Thus, this is not considered to be a major issue.
The significantly thinner support structure is a bigger issue. Since this space is used in order to assemble the strut, less available space can become an issue for the manufacturability of this strut.

Manufacturability

The thinner support structure was chosen in order to create a unit-cell system that was similar to the original strut in terms of dimensions and displacement capability. However, the thinner support structure could pose an issue for the manufacturability. Either another

assembly method must be studied in order to realise this exact strut or the strut must be designed again without taking the similarity with the original strut in mind. This could be done by either increasing the design space or by limiting the displacement capability of the unit-cell system.
However, in this paper it is assumed that the strut can be manufactured as is.

Another big part of the manufacturability of the unit-cell system is the added sensors and actuators. The sensors need to be implemented in the unit-cells and need to be read, and the actuators need to be controlled.
To solve this issue, the assumption that the strut is a perfect one-dimensional system is used. Using this property, the sensors can simply be added to the side of the unit-cells instead of inside the unit-cells. This means that the accelerometers are attached to the 'fingers' of the unit-cells. The sensors can now still be considered to be collocated since the system is considered one-dimensional.
As for the control of the actuators, the controllers will be separate from the strut. Thus, only the electrodes of the Piezo stack actuators need to have a connection to the outside world. For this, it is assumed that a similar approach can be used as the original system.

B Appendix B: Matlab Code

In this appendix, the various Matlab codes used for the theoretical derivation of the transmissibilities is presented.

ParametersUCS

Various parameter values used in further codes.

```
%% Control
PPI = 60000;
PUC = 30000;

%% Structural parameters
Uk = 2*((218/552.1553)*170e6); %1.0886e+08;
Uk3 = 3*((171.2568/552.1553)*170e6);
Uk5 = 132.5E6;
g = 0.1;
T = 0.5;
Ef = 0.5;
wf = 250*2*pi;
Mb = 1; %in kg
Ml = 80; %in kg

%% Dynamics of sensor
bwu = 5000; %in hz
DV = 2;
Te = 1/(DV*2*pi*bwu);

s0 = 1;
s1 = DV*Te;
s2 = DV*Te^2;

bwl = 1; %in hz
DV = 2;
Te2 = 1/(DV*2*pi*bwl);

h0 = 1;
h1 = DV*Te2;
h2 = DV*Te2^2;

%% Noise & Disturbance
Myseed = randi(100000,'double');
Myseed = 22020;
Dt = readtable('Example_disturbance_signal');

%% Blocking force
BF = [39000,44000,49000,50000];
LP = [33,58,105,154];
p = polyfit(LP,BF,2);
```

```
42 pn = @(x) p(1)*x.^2+p(2)*x+p(3);
```

TwoMassSystemDynamics

The code used for the theoretical transmissibility functions of the presented two mass-spring system that showed the working principle of the unit-cell interaction.

```
%Everything is defined with M*X*s^2 = F + K*X and separate cells (FBD of every cell)
%% Parameters
m1 = Mb;
m2 = Mb+Ml;
ml = Ml;
m = m1;
k1 = Uk;
k2 = Uk;
k = Uk;
%% Variables
syms F1 F2 x1 x2 s;
% syms m m1 m2 ml k k1 k2;
M = [m1 0; 0 m2];
K = [-k1-k2 k2; k2 -k2];
%F = [F1-F2; F2];
X = [x1; x2];
% sys = M*X*s^2 == F + K*X;
%% G11
syms F1 F2 x1 x2 s;
F = [1; 0];
X = [x1; x2];
sys = M*X*s^2 == F + K*X;
[x2] = solve(sys(1),x2);
X = [x1; x2];
sys = M*X*s^2 == F + K*X;
[G11] = solve(sys(2),x1);
%% G12
syms F1 F2 x1 x2 s;
F = [1; 0];
X = [x1; x2];
sys = M*X*s^2 == F + K*X;
[x1] = solve(sys(1),x1);
X = [x1; x2];
sys = M*X*s^2 == F + K*X;
[G12] = solve(sys(2),x2);
%% G21
syms F1 F2 x1 x2 s;
F = [-1; 1];
X = [x1; x2];
sys = M*X*s^2 == F + K*X;
[x2] = solve(sys(1),x2);
X = [x1; x2];
sys = M*X*s^2 == F + K*X;
[G21] = solve(sys(2),x1);
```

```
%% G22
syms F1 F2 x1 x2 s;
F = [-1; 1];
X = [x1; x2];
sys = M*X*s^2 == F + K*X;
[x1] = solve(sys(1),x1);
X = [x1; x2];
sys = M*X*s^2 == F + K*X;
[G22] = solve(sys(2),x2);
%% Gt
G12t = G12*k1; %Transmissibility uncontrolled system

syms kn d;
syms F1 F2 x1 x2 s;

d = 1;
kn = Uk*0.999; %Control gain

X = [x1; x2];
Gm = [G11, G21; G12, G22];
Ff = [k1*d; -x1*kn];
sysf = X == Gm*Ff;
[x1] = solve(sysf(1),x1);
Ff = [k1*d; -x1*kn];
X = [x1; x2];
sysf = X == Gm*Ff;
[Gt] = solve(sysf(2),x2);
Gt = simplify(Gt); %Transmissibility controlled system
```

ThreeMassSystemDynamics

The code used for the theoretical transmissibility functions of the presented three mass-spring system used for the validation comparison.

```
%Everything is defined with M*X*s^2 = F + K*X and separate cells
    (FBD of every cell)
%% Parameters
m1 = Mb;
m2 = Mb;
m3 = Mb+Ml;
ml = Ml;
m = m1;
k1 = Uk3;
k2 = Uk3;
k3 = Uk3;
k = Uk3;
%% Variables
syms F1 F2 F3 x1 x2 x3 s;
% syms m m1 m2 m3 ml k k1 k2 k3;
M = [m1 0 0; 0 m2 0; 0 0 m3];
K = [-k1-k2 k2 0; k2 -k2-k3 k3; 0 k3 -k3];
%F = [F1-F2; F2-F3; F3];
X = [x1; x2; x3];
% sys = M*X*s^2 == F + K*X;

%% G11
syms F1 F2 F3 x1 x2 x3 s;
F = [1; 0; 0];
X = [x1; x2; x3];
sys = M*X*s^2 == F + K*X;
[x2] = solve(sys(1),x2);
X = [x1; x2; x3];
sys = M*X*s^2 == F + K*X;
[x3] = solve(sys(2),x3);
X = [x1; x2; x3];
sys = M*X*s^2 == F + K*X;
[G11] = solve(sys(3),x1);
%% G12
syms F1 F2 F3 x1 x2 x3 s;
F = [1; 0; 0];
X = [x1; x2; x3];
sys = M*X*s^2 == F + K*X;
[x1] = solve(sys(1),x1);
X = [x1; x2; x3];
sys = M*X*s^2 == F + K*X;
[x3] = solve(sys(2),x3);
X = [x1; x2; x3];
sys = M*X*s^2 == F + K*X;
[G12] = solve(sys(3),x2);
```

```
%% G13
syms F1 F2 F3 x1 x2 x3 s;
F = [1; 0; 0];
X = [x1; x2; x3];
sys = M*X*s^2 == F + K*X;
[x1] = solve(sys(1),x1);
X = [x1; x2; x3];
sys = M*X*s^2 == F + K*X;
[x2] = solve(sys(2),x2);
X = [x1; x2; x3];
sys = M*X*s^2 == F + K*X;
[G13] = solve(sys(3),x3);
%% G21
syms F1 F2 F3 x1 x2 x3 s;
F = [-1; 1; 0];
X = [x1; x2; x3];
sys = M*X*s^2 == F + K*X;
[x2] = solve(sys(1),x2);
X = [x1; x2; x3];
sys = M*X*s^2 == F + K*X;
[x3] = solve(sys(2),x3);
X = [x1; x2; x3];
sys = M*X*s^2 == F + K*X;
[G21] = solve(sys(3),x1);
%% G22
syms F1 F2 F3 x1 x2 x3 s;
F = [-1; 1; 0];
X = [x1; x2; x3];
sys = M*X*s^2 == F + K*X;
[x1] = solve(sys(1),x1);
X = [x1; x2; x3];
sys = M*X*s^2 == F + K*X;
[x3] = solve(sys(2),x3);
X = [x1; x2; x3];
sys = M*X*s^2 == F + K*X;
[G22] = solve(sys(3),x2);
%% G23
syms F1 F2 F3 x1 x2 x3 s;
F = [-1; 1; 0];
X = [x1; x2; x3];
sys = M*X*s^2 == F + K*X;
[x1] = solve(sys(1),x1);
X = [x1; x2; x3];
sys = M*X*s^2 == F + K*X;
[x2] = solve(sys(2),x2);
X = [x1; x2; x3];
sys = M*X*s^2 == F + K*X;
[G23] = solve(sys(3),x3);
%% G31
```

```
94  syms F1 F2 F3 x1 x2 x3 s;
95  F = [0; -1; 1];
96  X = [x1; x2; x3];
97  sys = M*X*s^2 == F + K*X;
98  [x2] = solve(sys(1),x2);
99  X = [x1; x2; x3];
100 sys = M*X*s^2 == F + K*X;
101 [x3] = solve(sys(2),x3);
102 X = [x1; x2; x3];
103 sys = M*X*s^2 == F + K*X;
104 [G31] = solve(sys(3),x1);
105 %% G32
106 syms F1 F2 F3 x1 x2 x3 s;
107 F = [0; -1; 1];
108 X = [x1; x2; x3];
109 sys = M*X*s^2 == F + K*X;
110 [x1] = solve(sys(1),x1);
111 X = [x1; x2; x3];
112 sys = M*X*s^2 == F + K*X;
113 [x3] = solve(sys(2),x3);
114 X = [x1; x2; x3];
115 sys = M*X*s^2 == F + K*X;
116 [G32] = solve(sys(3),x2);
117 %% G33
118 syms F1 F2 F3 x1 x2 x3 s;
119 F = [0; -1; 1];
120 X = [x1; x2; x3];
121 sys = M*X*s^2 == F + K*X;
122 [x1] = solve(sys(1),x1);
123 X = [x1; x2; x3];
124 sys = M*X*s^2 == F + K*X;
125 [x2] = solve(sys(2),x2);
126 X = [x1; x2; x3];
127 sys = M*X*s^2 == F + K*X;
128 [G33] = solve(sys(3),x3);
129
130 %% Gt
131 G13t = k1*G13;  %Transmissibility uncontrolled system
132
133 syms kn d P1 P2 P3;
134 syms F1 F2 F3 x1 x2 x3 s;
135
136 d = 1;
137 kn = k2; %0.9999 %Control gain
138 P1 = 0.5*PUC; %DVF-gain first controller
139 P2 = 0.5*PUC; %DVF-gain second controller
140 P3 = 2*PUC;   %DVF-gain third controller
141
142 X = [x1; x2; x3];
```

```
143 Gm = [G11, G21, G31; G12, G22, G32; G13, G23, G33];
144 Ff = [k1*d-s*P1*x1; -x1*kn-s*P2*x2; -s*P3*x3];
145 sysf = X == Gm*Ff;
146 [x1] = solve(sysf(1),x1);
147 Ff = [k1*d-s*P1*x1; -x1*kn-s*P2*x2; -s*P3*x3];
148 X = [x1; x2; x3];
149 sysf = X == Gm*Ff;
150 [x2] = solve(sysf(2),x2);
151 x1 = subs(x1,x2);
152 Ff = [k1*d-s*P1*x1; -x1*kn-s*P2*x2; -s*P3*x3];
153 X = [x1; x2; x3];
154 sysf = X == Gm*Ff;
155 [Gt] = solve(sysf(3),x3);
156 Gt = simplify(Gt); %Transmissibility controlled system
```

syms2tf

The code used to convert a symbolic expression with the Laplace variable to a transfer function to be used with the 'bode' command. It is important to ensure the symbolic expression has only one numerator and one denominator in the entire expression.

```
function [Gs] = syms2tf(G)
[symNum,symDen] = numden(G); %Get num and den of Symbolic TF
TFnum = sym2poly(symNum);    %Convert Symbolic num to polynomial
TFden = sym2poly(symDen);    %Convert Symbolic den to polynomial
Gs =tf(TFnum,TFden);
end
```